1

Introduction

During the life of a structure, impacts by foreign objects can be expected to occur during manufacturing, service, and maintenance operations. An example of in-service impact occurs during aircraft takeoffs and landings, when stones and other small debris from the runway are propelled at high velocities by the tires. During the manufacturing process or during maintenance, tools can be dropped on the structure. In this case, impact velocities are small but the mass of the projectile is larger. Laminated composite structures are more susceptible to impact damage than a similar metallic structure. In composite structures, impacts create internal damage that often cannot be detected by visual inspection. This internal damage can cause severe reductions in strength and can grow under load. Therefore, the effects of foreign object impacts on composite structures must be understood, and proper measures should be taken in the design process to account for these expected events. Concerns about the effect of impacts on the performance of composite structures have been a factor in limiting the use of composite materials. For these reasons, the problem of impact has received considerable attention in the literature. The objective with this book is to present a comprehensive view of current knowledge on this very important topic.

A first step in gaining some understanding of the problem is to develop mathematical models for predicting the force applied by the projectile on the structure during impact. In order to predict this contact force history, the model should account for the motion of the structure, the motion of the projectile, and the local deformations in the contact zone. A detailed description of the contact between the impactor and the structure during impact would be difficult to obtain and is not required as part of the impact dynamics analysis. Instead, what is needed is a contact law relating the contact force to the indentation, which is defined as the motion of the projectile relative to that of the target. With the material systems commonly used, strain rate effects are negligible such

that static and dynamic contact laws are identical, and so statically determined contact laws can be used in the dynamics analysis. Many investigators analyzed the loading phase of the indentation process and predicted the contact law for beams and plates with various boundary conditions and several indentor shapes. The indentation process introduces damage and permanent deformations in the contact zone; as a result, the unloading curve differs from the loading curve. In many cases, multiple impacts occur and the reloading curve is again different. While some simple analyses of the unloading and reloading phases have been presented, a complete and accurate characterization of the contact law for a particular target–indentor combination can only be obtained experimentally. A set of equations are commonly used to describe the contact behavior between solid laminates and smooth indentors, with a small number of constants to be determined from experiments. Contact problems are discussed in Chapter 2.

An important aspect of a model for predicting the impact dynamics is to accurately describe the dynamic behavior of the target. For some simple cases, the motion of the structure can be modeled by a simple spring–mass system or by assuming a quasi-static behavior and considering the balance of energy in the system. But in general, more sophisticated beam, plate, or shell theories are required to model the structure. Two- and three-dimensional elasticity models are also employed. For each particular case, a choice must be made between a number of theories developed to account for complicating factors such as transverse shear deformation and rotary inertia. In addition, one must select to use variational approximation methods or finite element methods if exact solutions are not available for the case at hand. In Chapter 3, several structural theories are presented and their accuracies are discussed, particularly in regard to the impact problem. Several examples of impact dynamics analyses are presented for impacts on beams, plates, and shells. Often tests cannot be performed on full scale prototypes, so small specimens must be used. In other cases, tests or analyses have been performed on two specimens of different sizes. Methods developed to scale results obtained from a small-scale model to a full-size prototype are discussed in Chapter 3.

Different test apparatus are used to simulate various types of impact. Drop-weight testers are used to simulate low-velocity impacts typical of the tool-drop problem, in which a large object falls onto the structure with low velocity. Air-gun systems, in which a small projectile is propelled at high speeds, are used to simulate the type of impacts encountered during aircraft takeoffs and landings. Testing conditions should replicate the actual impacts the structure is designed to withstand, and so the choice of the proper test apparatus is important. Descriptions of several common types of impact testers are given in Chapter 4, where damage development, the morphology of impact damage,

and experimental techniques for damage detection are also described. Impact damage consists of delaminations, matrix cracking, and fiber failure. Extensive experimental investigations have revealed definite patterns for the shape of the damage and its initiation and growth. It is generally accepted that during low-velocity impacts, damage is initiated by matrix cracks which create delaminations at interfaces between plies with different fiber orientations. For stiff structures, matrix cracks start on the impacted face of the specimen due to high contact stresses. Damage propagates downward by a succession of intra-ply cracks and interface delaminations to give what is called a pine tree pattern. For thin specimens, bending stresses cause matrix cracking in the lowest ply, and damage progresses from the nonimpacted face up toward the projectile giving a reverse pine tree appearance. Many studies demonstrated that no delaminations are induced at the interface between plies with the same fiber orientation. The delaminated area at an interface depends on the fiber orientations in the plies adjacent to that interface. Of the large number of experimental methods that have been developed for damage assessment, some result in the complete destruction of the specimen and others are nondestructive, but most methods are used to determine the state of damage after impact. A few methods can be used to monitor the development of damage during impact. Once the failure modes involved are known and methods to assess damage are available, the next task is to determine what the governing parameters are. The properties of the matrix, the reinforcing fibers, and the fiber–matrix interfaces affect impact resistance in several ways, along with effects of layup, thickness, size, boundary conditions, and the shape, mass, and velocity of the projectile. Techniques for improving both impact resistance and impact tolerance will also be discussed.

The prediction of impact damage is a difficult task for which complete success may not be possible and is probably not necessary. A large number of matrix cracks and delaminations are created in the impact zone, and the introduction of each new crack creates a redistribution of stresses. Thus it is not realistic to attempt to track every detail of damage development during the dynamic analysis of the impact event. Some purely qualitative models explain the orientation and size of delaminations at the various interfaces through the thickness of the laminate. Other models predict the onset of delaminations by predicting the appearance of the first matrix crack. Models for estimating the final state of delaminations are available. Chapter 5 deals with models for predicting impact damage.

Impact-induced delaminations result in drastic reductions in strength, stiffness, and stability of the laminate, which explains why impact is of such concern to the designers and users of composite structures and why such effort has been directed at understanding the problem. Reductions are particularly significant

in compression, where the effect of delaminations is more readily visible. The extent of these reductions has been characterized experimentally, and several mathematical models are used to predict the residual strength, as discussed in Chapter 6.

Chapter 7 deals with high-velocity impacts. Sometimes the expression "high-velocity impact" refers to impacts resulting in complete perforation of the target. However, it must be recognized that complete perforation can be achieved both under low-velocity impacts when overall deflections of the target are taking place and under high-velocity impacts when the deformations of the target are localized in a small region near the point of impact. Here, high-velocity impacts are defined so that the ratio between impact velocity and the velocity of compressive waves propagating through the thickness is larger than the maximum strain to failure in that direction. This implies that damage is introduced during the first few travels of the compressive wave through the thickness when overall plate motion is not yet established. The ballistic limit is defined as the initial velocity of the projectile that results in complete penetration of the target with zero residual velocity. For impact velocities above the ballistic limit, the residual velocity of the projectile is also of interest. General trends for ballistic impacts (including the effect of several important parameters) are known from experimental results, and models for predicting the ballistic limit are available. Another area to be discussed in this chapter is the design of composite armor, which usually involves using one layer of ceramic material to blunt or fragment the projectile and another layer of composite material to absorb the residual kinetic energy.

Many repair procedures for composite structures with impact damage have been reported. In selecting a particular repair technique, several factors must be considered, including the severity of the damage, the loads to be sustained, and the equipment available at the location where the repair procedure will be performed. In some cases, a successful repair cannot be made and the part must be replaced. In other cases, only cosmetic repairs are needed. In yet other cases, either bolted repairs or bonded repairs are needed. Proper design of the repair patch, machining, surface preparation, prefabrication of patches, and bonding are important phases of a successful repair procedure. The basic problems and most promising approaches are reported in Chapter 8.

In many applications, sandwich structures with laminated facings are used because of the well-known advantages of this type of construction. The facings are loaded primarily in tension or compression to resist bending while the core resists the shear stresses. As a result, sandwich structures achieve a great bending rigidity, but in the transverse direction the rigidity remains low. A low rigidity in the transverse direction results in a low contact stiffness and

lower contact forces during impact. Contact laws for sandwich structures are completely different from those of monolithic laminates and are dominated by the deformation of the core. Usually cores are made out of honeycomb materials, foam, or balsa wood. All these materials are considered to be part of the family of cellular materials and have a similar stress–strain behavior when loaded in compression in the transverse direction. The choice of a particular material is based on considerations of performance, weight, and cost. Models for predicting the behavior of a sandwich panel under a smooth indentor are discussed in Chapter 9. Impact creates damage to the facings, the core, and the core-facing interfaces. The evolution of damage with impact energy and its effects on the residual properties of sandwich panels are also discussed in that chapter.

2

Contact Laws

2.1 Introduction

Local deformations in the contact region must be accounted for in the analysis in order to accurately predict the contact force history. The indentation, defined as the difference between the displacement of the projectile and that of the back face of the laminate, can be of the same order as or larger than the overall displacement of the laminate. One could consider the projectile and the structure as two solids in contact and then analyze the impact problem as a dynamic contact problem. However, this approach is computationally expensive and cannot describe the effect of permanent deformation and local damage on the unloading process. The unloading part of the indentation process can be modeled only using experimentally determined contact laws. To predict the contact force history and the overall deformation of the target, a detailed model of the contact region is not necessary. A simple relationship between the contact force and the indentation, called the *contact law*, has been used by Timoshenko (1913) to study the impact of a beam by a steel sphere. This approach has been used extensively since then and is commonly used for the analysis of impact on composite materials.

Although the impact event is a highly dynamic event in which many vibration modes of the target are excited, statically determined contact laws can be used in the impact dynamics analysis of low-velocity impacts because strain rate and wave propagation effects are negligible with commonly used material systems. Hunter (1957) calculated the energy lost by elastic waves during the impact of a sphere on an elastic half-space. The ratio between the energy lost in the half-space and the initial kinetic energy of the sphere is given by

$$1.04\left(\frac{V}{(E/\rho)^{\frac{1}{2}}}\right)^{\frac{3}{5}}. \tag{2.1}$$

Therefore, the energy loss is negligible as long as the initial velocity of the

sphere, V, is small compared with $c = (E/\rho)^{1/2}$, the phase velocity of compressive elastic waves in the solid. In many cases, the contact area is small and the behavior is similar to that observed during the indentation of a half-space. The indentation is independent of the overall deflection of the structure. When the contact area becomes large, the overall deflection of the structure affects the pressure distribution under the indentor; this interaction must be accounted for accurately.

This chapter presents the basic results from contact mechanics needed to model the indentation of composite materials during the impact by a foreign object. The objective of such models is the accurate prediction of the contact force history and the overall response of the structure.

2.2 Contact between Two Isotropic Elastic Solids

Detailed accounts of the study of contact between two smooth elastic solid pioneered by Hertz are given in several books (Barber 1992, Gladwell 1980, Johnson 1985, Timoshenko and Goodier 1970). Essential results from Hertz theory of contact as given here without derivation. For two isotropic bodies of revolution (Fig. 2.1), contact occurs in a circular zone of radius a in which the normal pressure p varies as

$$p = p_0 \left[1 - \left(\frac{r}{a} \right)^2 \right]^{\frac{1}{2}} \tag{2.2}$$

where p_0 is the maximum contact pressure at the center of the contact zone and r is the radial position of an arbitrary point in the contact zone (Fig. 2.2). Defining the parameters R and E as

$$\frac{1}{R} = \frac{1}{R_1} + \frac{1}{R_2}, \tag{2.3}$$

$$\frac{1}{E} = \frac{1 - \nu_1^2}{E_1} + \frac{1^2 - \nu_2^2}{E_2} \tag{2.4}$$

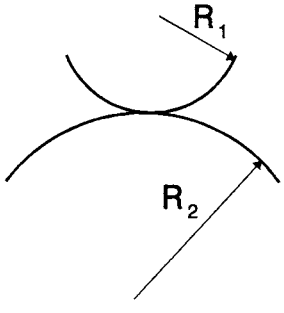

Figure 2.1. Two bodies of revolution for Hertzian analysis of contact.

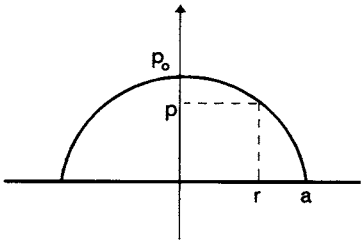

Figure 2.2. Pressure distribution in the contact zone.

where R_1 and R_2 are the radii of curvature of the two bodies. The Young moduli and Poisson's ratios of the two bodies are E_1, ν_1, and E_2, ν_2, respectively. Without loss of generality, the subscript 1 is taken to denote properties of the indentor and subscript 2 identifies properties of the target. The radius of the contact zone a, the relative displacement α, and the maximum contact pressure are given by

$$a = \left(3\frac{PR}{4E}\right)^{\frac{1}{3}} \tag{2.5}$$

$$\alpha = \frac{a^3}{R} = \left(\frac{9P^2}{16RE^2}\right)^{\frac{1}{3}} \tag{2.6}$$

$$p_0 = \frac{3P}{2\pi a^2} = \left(\frac{6PE^2}{\pi^3 R^2}\right)^{\frac{1}{3}}. \tag{2.7}$$

The force indentation law is expressed as

$$P = k\alpha^{\frac{3}{2}} \tag{2.8}$$

where P is the contact force, α is the indentation, and the contact stiffness k is given by

$$k = \frac{4}{3}ER^{\frac{1}{2}}. \tag{2.9}$$

Equation (2.8) is usually referred to as *Hertz contact law* or the *Hertzian law of contact* and is found to apply for a wide range of cases, even if all the assumptions made in the derivation of the theory are not satisfied. For example, (2.8) also applies for laminated composites, even though these are not homogeneous and isotropic materials. With composite materials, permanent deformations are introduced in the contact zone for relatively low force levels, but the material is assumed to remain linear elastic in the analysis. Matrix cracks, fiber fracture, and interply delaminations can be introduced in the contact zone, but overall the contact law follows (2.8).

The experimental determination of the contact law usually involves the use of a displacement sensor which directly measures the displacement of the indentor relative to the back face of the specimen. The plot of the applied force versus the indentation measured in this way follows the general form given by (2.8). Least-squares fits of the experimental data usually show that the exponent of α in that equation is close to $\frac{3}{2}$, and k is close to the value given by (2.9). Some investigators present plots of the contact force versus the displacement of the indentor that show a significant discontinuity when delaminations are introduced. The displacement of the indentor is the sum of the indentation and the deflection of the structure. The observed discontinuity corresponds to the reduction in the apparent stiffness of the structure caused by the introduction of delaminations.

2.3 Indentation of Beams

During the indentation of beams, local deformations are superposed onto the overall deflection of the beam. When the beam deflections are small, the interaction between the local indentation and the overall deflection of the beam is negligible. Therefore, the indentation law and the pressure distribution in the contact zone are the same as for the indentation of a half-space. However, for flexible beams under large indentors, the beam may wrap around the indentor, leading to significant changes in the normal pressure distribution.

First, consider the bending of a Bernoulli-Euler beam and neglect local deformations. This simple analysis will provide some understanding of the physical behavior of a beam loaded by a large indentor. From the free body diagram of an infinitesimal beam element (Fig. 2.3), the equilibrium equations for a planar beam are

$$\frac{dV}{dx} + p = 0, \quad \frac{dM}{dx} + V = 0, \tag{2.10}$$

where V is the shear force, M is the bending moment, and p is the applied force per unit length. With the Bernoulli-Euler beam theory, plane sections are assumed to remain planar and perpendicular to the neutral axis of the beam.

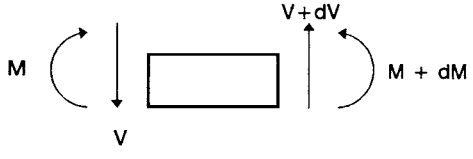

Figure 2.3. Free body diagram of beam element.

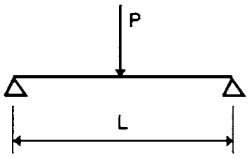

Figure 2.4. Simply supported beam with concentrated force applied in center.

The axial displacements are then related to the transverse displacement by

$$u(x,z) = -z\frac{dw(x)}{dx}, \tag{2.11}$$

and the axial strain is

$$\epsilon_{xx} = -z\frac{d^2w}{dx^2}. \tag{2.12}$$

The bending moment is related to the transverse displacement by

$$\begin{aligned} M &= -\int_A \sigma_{xx} z dA = -\int_A E\epsilon_{xx} z dA \\ &= E\int_A z^2 dA \frac{d^2w}{dx^2} = EI\frac{d^2w}{dx^2}. \end{aligned} \tag{2.13}$$

The bending moment distribution in a simply supported beam of length L subjected to a concentrated force applied in the center (Fig. 2.4) is given by

$$M = \frac{P}{2}\left(\frac{L}{2} - x\right) \tag{2.14}$$

for $x > 0$. The curvature of the beam is given by the second derivative of the deflection. Using (2.13) and (2.14), the load required to bend the beam to a radius R equal to that of the indentor is found to be

$$P = 4\frac{EI}{RL}, \tag{2.15}$$

which indicates that wrapping is more likely to occur for long flexible beams under a large impactor.

As the load increases, the beam comes in contact with the indentor over a distance a (Fig. 2.5). In that region, the radius of curvature is constant and equal to the radius of the impactor. Equation (2.13) implies that the bending moment is also constant, and (2.10) indicates that the shear force is uniformly equal to zero and that the pressure under the impactor is also zero. The beam is then loaded by two concentrated forces of magnitude $P/2$ located at $+a$ and $-a$. The distance a is such that the curvature of the beam at $x = a$ is equal to the